ACal™

Innovation, Research & Development
Radiometrics Corp.

May 4, 2022

1 Introduction

1.1 A Novel Automatic Calibration Process for Microwave Radiometers

Radiometrics has developed cryogenic-free automatic calibration process (ACal™) that eliminates the need for regular liquid nitrogen (LN) calibration of the microwave radiometer profilers. Radiometrics has extensively tested the ACal methodology over a number of years and verified that ACal is equivalent or superior to specified LN calibration accuracy as shown in Table 1. In all cases, ACal improved the instrument calibration when compared to LN calibration, as validated by brightness temperature comparisons with forward modeled radiosonde data.

1.2 Results

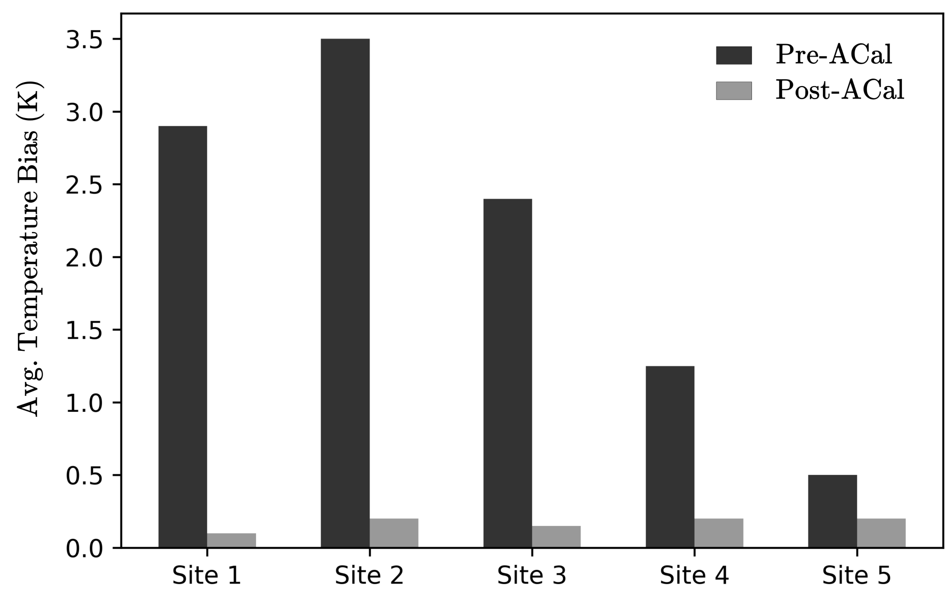

Figure 1: ACal demonstrates significantly improved temperature accuracy statistics compared to liquid nitrogen calibration methods when compared to radiosondes.

Alias	Location	Period (Days)	Pre-ACal Bias (K)	Post-ACal Bias (K)
Site 1	Germantown, MD	365	2.9	0.1
Site 2	Cape Canaveral, FL	120	3.5	0.2
Site 3	San Jose, CA	575	2.7	0.2
Site 4	Albany, NY	14	1.3	0.2
Site 5	Boulder, CO	180	0.5	0.2

Table 1: ACal comparative analysis site information and performance improvement metrics.

1.3 Comparative Advantages as Compared to Liquid Nitrogen (LN) Calibration

- ACal can be user-configured to continuously evaluate and update calibration, vs. periodic calibration.
- ACal eliminates any errors due to target reflections, water/ice condensation/freezing in humid conditions, or operator error.
- ACal provides an additional level of instrument health monitoring, and can aid in identifying instrument servicing is needed before a hard failure occurs.
- ACal eliminates the need for LN, and for an operator to visit the instrument location to conduct the calibration.
- ACal is an always-on measurement accuracy assurance system, providing quantitative calibration metrics to inform measurement confidence.

2 ACal

ACal is a composite calibration method that relies on various independent subroutine calibrations tailored to specific operational frequency bands of the radiometer. Each of the calibration methods is tailored to calibrate a specific frequency band of the radiometer. In each subroutine calibration, the generalized calibration algorithm is utilized.

2.1 Generalized Theory

To accurately process the integrated receiver signal, the radiation temperature of the emitter must be known or inferred. Whereas the blackbody target effective radiation temperature is directly measured, the effective radiation temperature of emitters in the sky measurement ($\boldsymbol{T_{\mathbf{sky}}}$) is not directly measured. As such - whether by proxy measurement, inference, or statistical mechanics - $\boldsymbol{T_{\mathbf{sky}}}$ must be assigned as a forcing parameter to define the calibration fitting parameters.

Assigning effective radiation temperatures to $\boldsymbol{T_{\mathbf{sky}}}$ imposes a relationship between the measured values: $\boldsymbol{V_{\mathbf{sky}}}$, $\boldsymbol{V_{\mathbf{sky_{nd}}}}$, $\boldsymbol{V_{\mathbf{bb}}}$, $\boldsymbol{V_{\mathbf{bb_{nd}}}}$, & $\boldsymbol{Tk_{\mathbf{bb}}}$. Once the relationship between the measured values has been imposed by assignment of the effective radiation temperature of $\boldsymbol{T_{\mathbf{sky}}}$, the Calibration Parameters - $\boldsymbol{\alpha}$, $\mathbf{Tnd_{290}}$, $\boldsymbol{K1-K4}$, & $\boldsymbol{dTdG}$ - may be re-fit through the process of nonlinear least-squares regression to populate the thermally-dependent calibration surface.

2.2 Definitions

2.2.1 Measured Values

- $\boldsymbol{V_{\mathbf{sky}}}$: Integrated receiver output voltage from a sky observation with noise diode **off**
- $\boldsymbol{V_{\mathbf{sky_{nd}}}}$: Integrated receiver output voltage from a sky observation with noise diode **on**
- $\boldsymbol{V_{\mathbf{bb}}}$: Integrated receiver output voltage from a ambient blackbody target observation with noise diode **off**

- $\boldsymbol{V_{\mathrm{bb_{nd}}}}$: Integrated receiver output voltage from a ambient blackbody target observation with noise diode **on**
- $\boldsymbol{Tk_{\mathrm{bb}}}$: Blackbody target effective radiation temperature

2.2.2 Calibration Parameters

- $\boldsymbol{\alpha}$: Non-linearity correction exponent
- $\boldsymbol{T\mathrm{nd}_{290}}$: Noise diode temperature when $Tk_{\mathrm{bb}} = 290$ Kelvin
- $\boldsymbol{K1 - K4}$: Temperature coefficients
- $\boldsymbol{dTdG}$: Receiver hardware-specific parameter

2.2.3 Calculated Values

$$\mathrm{T_{sky}} = \left(\frac{V_{\mathrm{sky}}}{\mathrm{Gain_{sky}}}\right)^{\frac{1}{\alpha}} - \mathrm{Trcv_{sky}} \tag{1}$$

$$\mathrm{Gain_{sky}} = \left(\frac{V_{\mathrm{sky_{nd}}}^{\frac{1}{\alpha}} - V_{\mathrm{sky}}^{\frac{1}{\alpha}}}{T\mathrm{nd}_{290} + TC}\right)^{\alpha} \tag{2}$$

$$\mathrm{Trcv_{sky}} = T\mathrm{rcv_{bb}} + dTdG\left(\mathrm{Gain_{sky}} - \mathrm{Gain_{bb}}\right) \tag{3}$$

$$\mathrm{Gain_{bb}} = \left(\frac{V_{\mathrm{bb_{nd}}}^{\frac{1}{\alpha}} - V_{\mathrm{bb}}^{\frac{1}{\alpha}}}{T\mathrm{nd}_{290} + TC}\right)^{\alpha} \tag{4}$$

$$\mathrm{Trcv_{bb}} = \left(\frac{V_{\mathrm{bb}}}{\mathrm{Gain_{bb}}}\right)^{\frac{1}{\alpha}} - Tk_{\mathrm{bb}} \tag{5}$$

$$TC = K1 + K2 \cdot Tk_{\mathrm{bb}} + K3 \cdot Tk_{\mathrm{bb}}^2 + K4 \cdot Tk_{\mathrm{bb}}^3 \tag{6}$$

2.3 General Considerations and Constraints

2.3.1 Thermal Range

The temperature coefficient variable TC characterizes the radiometer's thermo-electric and thermo-mechanical response. As such, ACal maximizes the thermal range of calibration data; limited thermal ranges have the effect of truncating the thermally-dependent calibration surface as is observable with liquid nitrogen (LN) field calibration. While there is no intrinsic error in defining narrow thermal calibration ranges, confidence in measurement degrades as the operational thermal range of the radiometer deviates from the thermal range included in the calibration data. In general, maximizing the thermal range of measurement data is preferred. Figures 2 and 3 further develop the shortcomings of reduced thermal ranges associated with LN field calibration.

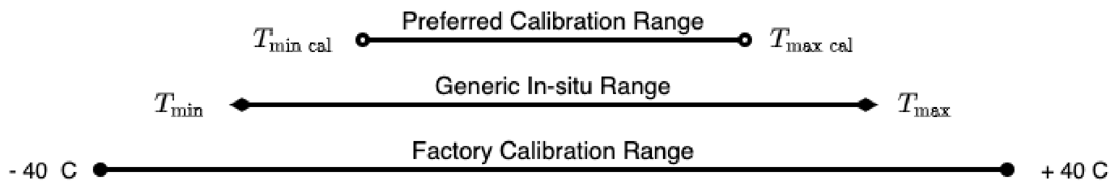

Figure 2: Generic relative thermal ranges are shown.

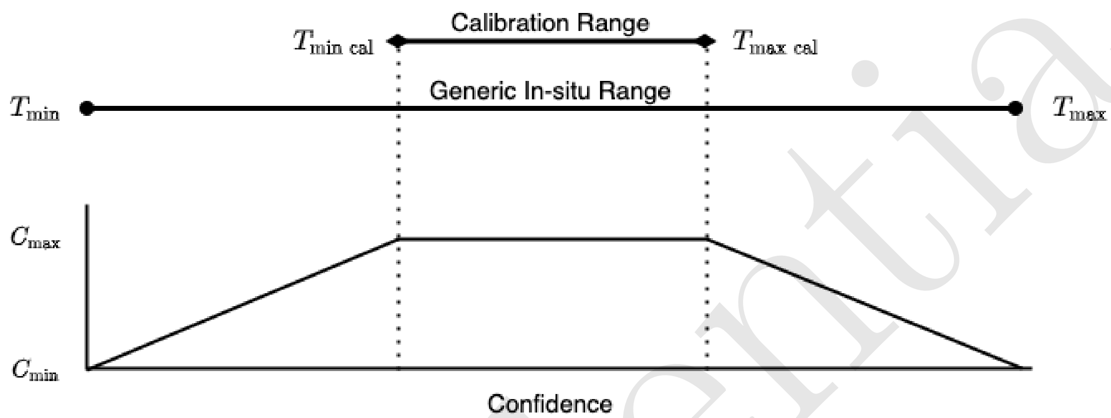

Figure 3: Measurement confidence degradation as a function of operational thermal range migration from calibration thermal range.

2.4 Validation and Verification of Calibration Performance

The fundamental radiometer measurement is the effective radiating temperature (brightness temperature; T_b), $\boldsymbol{T_{\mathrm{sky}}}$. As such, calibration validation and verification is properly applied via comparisons to forward-modeled T_bs.

2.4.1 Radiative Transfer & Forward Modeling

Atmospheric thermodynamic soundings (radiosondes) are forward-modeled to characteristic brightness temperatures via radiative transfer modeling as shown in Figure 4.

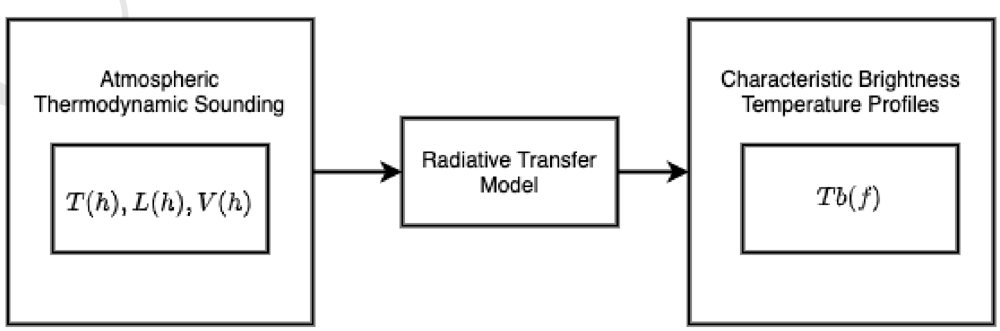

Figure 4: Forward modeling process is shown.

Treating radiosonde observations as a comparison truth source legitimizes the treatment of forward-modeled brightness temperatures as an analogous comparison truth source for the purposes of radiometer calibration validation and verification. Calibrated radiometer measurements will proximate brightness temperatures resulting from forward-modeled localized radiosondes (Figure 4).

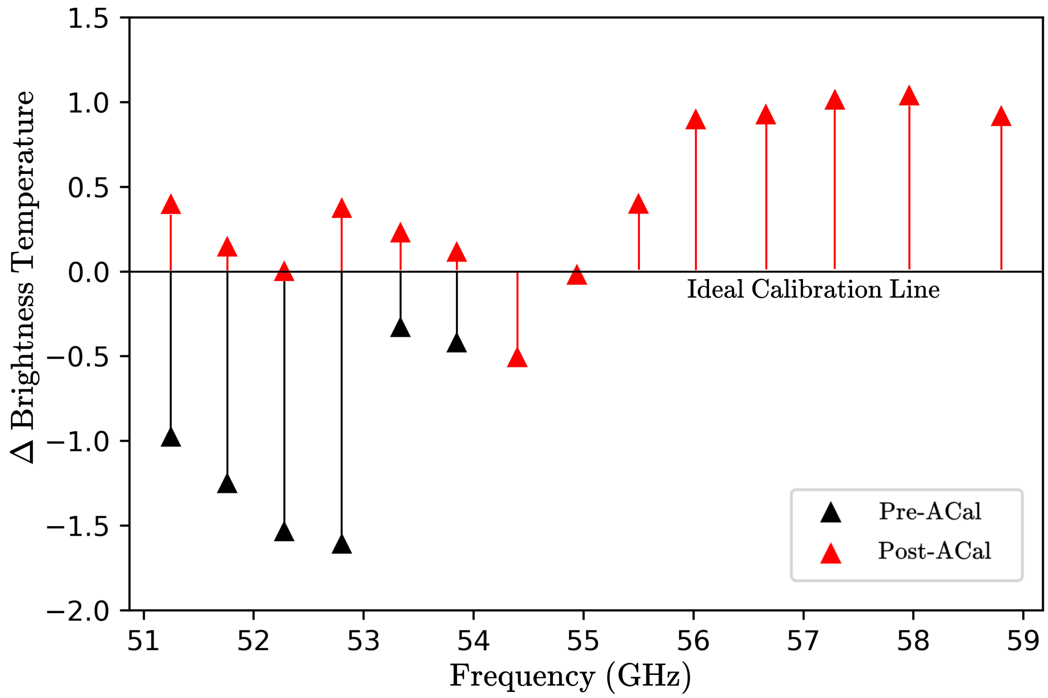

Figure 5: Forward-modeled minus measured Tb shows reduced ACal bias.

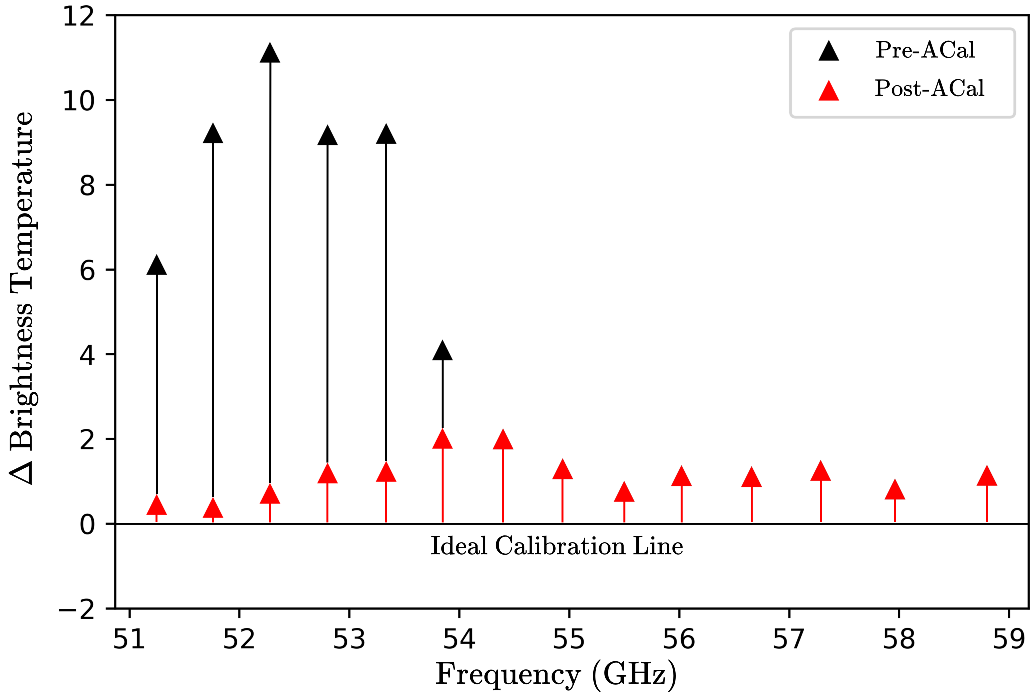

Figure 6: Forward-modeled minus measured Tb shows reduced ACal bias.

Figure 5 (Site 5; Boulder, CO) and Figure 6 (Site 3; San Jose, CA) demonstrate the superior performance of ACal (Post-ACal) - as compared to LN calibration (Pre-ACal) - in its ability to accurately resolve forward-modeled brightness temperatures[1,2]. Figure 6 demonstrates the tendency of radiometers to undergo calibration drift as a function of sustained absence of LN calibration, whereas Figure 5 shows reduced - but appreciable - LN calibration-associated under-performance when compared to ACal calibration.

2.4.2 Imposing ACal -derived $T_{\mathbf{sky}}$

Figure 6 demonstrates the significant discrepancies between radiometer brightness temperature measurements for pre- and post-ACal calibration configurations. Imposing ACal -derived T_{sky} onto the system of calibration equations has the effect of average bias reduction shown in Figure 1, Site 3.

All measured quantities from the radiometer measurement series are preserved, ACal-derived T_bs are imposed on the system of calibration equations, and new fitting parameters are assigned based on error minimization during nonlinear least-squares regression fitting.

[1]Figures 5 and 6 exhibit the calibration of the V-band receiver. K-band tipping is acknowledged in the literature as a high-accuracy calibration method. ACal utilizes Radiometrics proprietary automated TipCal algorithm to calibrate the k-band receiver.

[2]The statistical comparison in Figure 5 is associated with Boulder, CO (Site 5 from Figure 1) where the radiometer installation site was 30-km distance from the comparison radiosonde launch site in Denver, CO. The statistical comparison in Figure 6 is associated with San Jose, CA (Site 2 from Figure 1) where the radiometer installation site was 80-km distance from the comparison radiosonde launch site in Oakland, CA.

2.5 ACal as a Radiometer Accuracy Assurance System

For calibrated radiometers, the measured brightness temperatures will exhibit consistency with the ACal-derived brightness temperatures. When measured brightness temperatures exhibit consistency with ACal-derived brightness temperatures, ACal serves as a radiometer accuracy assurance system. From Figure 1, Site 5 data is associated with Radiometrics research and development radiometer, which undergoes frequent LN calibrations to assist with product engineering efforts. Notice the reduced average temperature bias associated with Site 5 and how ACal further reduces the average temperature bias. A statistical analysis of the differences between measured brightness temperatures and ACal-derived brightness temperatures demonstrates strong correlation throughout the 180-day measurement period, as shown in Figure 7.

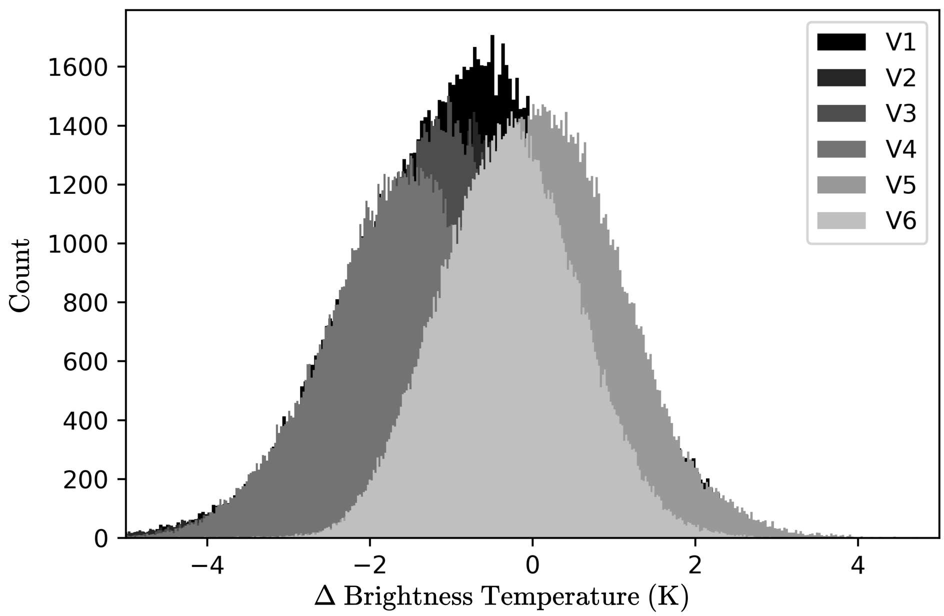

Figure 7: Distribution of measured vs. ACal-derived brightness temperatures.

The distribution of measured versus ACal-calibrated brightness temperatures exhibit non-zero peaks as the comparison radiosonde in Denver is 30-km distance away from the Boulder radiometer installation site. The statistical manifestation of the non-zero peaks is reflected in Figure 7.

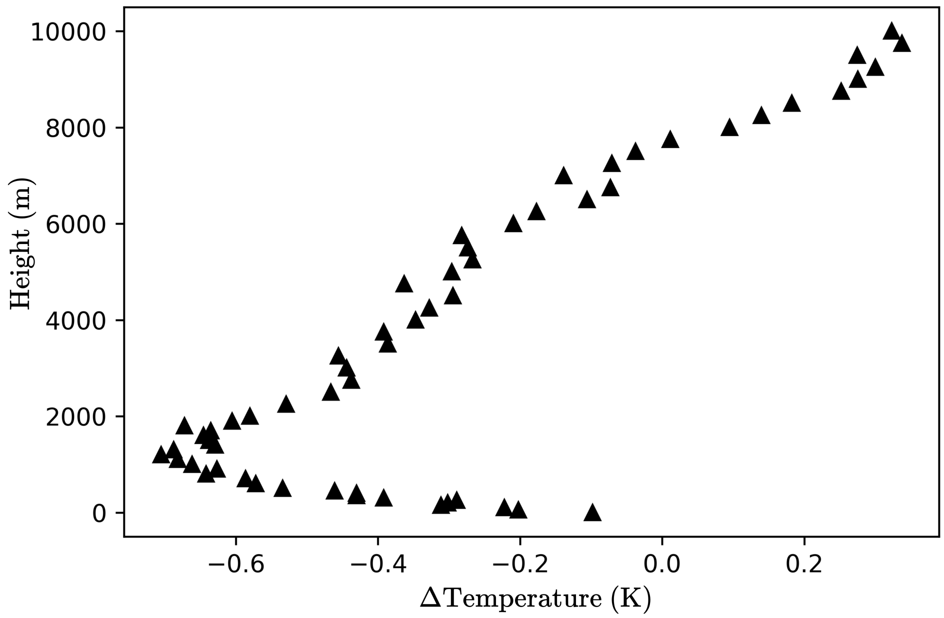

Figure 8: Average temperature bias improvement vs. height.

Figure 8 quantifies the height-resolved average bias accuracy improvements, which remain within the specified temperature accuracy range. When measured brightness temperatures agree with ACal-derived brightness temperatures, ACal remains in a monitoring status and refrains from initializing a re-calibration until the implied average temperature biases exceed the specified temperature accuracy range.